APEM journal
Advances in Production Engineering & Management
Volume 17 | Number 1 | March 2022 | pp 89–107
https://doi.org/10.14743/apem2022.1.423
ISSN 1854-6250
Journal home: apem-journal.org
Original scientific paper

A gold nanoparticles and hydroxylated fullerene water complex as a new product for cosmetics

Rudolf, R.[a,b,*], **Jelen, Ž.**[a], **Zadravec, M.**[a], **Majerič, P.**[a,b], **Jović, Z.**[c], **Vuksanović, M.**[c], **Stankovic, I.**[d], **Matija, L.**[d], **Dragičević, A.**[d], **Miso Thompson, N.**[e], **Horvat, A.**[f], **Koruga, D.**[c,d]

[a]University of Maribor, Faculty of Mechanical Engineering, Slovenia
[b]Zlatarna Celje d.o.o., Celje, Slovenia
[c]TFT Nano Center, Belgrade, Serbia
[d]University of Belgrade, Nano Lab, Faculty of Mechanical Engineering, Serbia
[e]ZeptoHyperTech, Belgrade, Serbia
[f]Zepter-Slovenica d.o.o., Slovenj Gradec, Slovenia

ABSTRACT

Three types of gold nanoparticles (AuNPs) were synthesised with a custom-made Ultrasonic Spray Pyrolysis (USP) device, from aqueous solutions of gold (III) chloride ($AuCl_3$) and gold (III) acetate ($AuC_6H_{12}O_6$), with an initial concentration of Au 0.5 g/L. AuNPs were collected in suspensions of deionised (D.I.) water with the stabilisers polyvinylpyrrolidone (PVP) or polyethylene glycol (PEG), followed by the process of freeze drying the AuNPs to be useful as a new additive for the cream. The standard cream base was used as a matrix for preparation of three types of cream with AuNPs in the same concentration ratios. The third AuNPs cream was prepared with a patented hydroxylated fullerene water complex (3HFWC-W) matrix. To examine the effect of AuNPs as additive in creams, a six-week study of test creams was conducted on 33 volunteers with no dermatological diseases. During the study three main parameters of the skin where measured: Collagen quality, skin moisturisation and the epidermis-dermis function. The results of the study found improvements of collagen quality between 18-24 %, achieved due to the use of AuNPs in standard creams, while the cream with the combination of 3HFWC-W and AuNPs gave significantly higher improvements with a value of 45.7 %. It was also discovered that hydration of the skin (stratum cornum) increased by 6.4-9.6 % in standard creams with AuNPs, and 73.7 % in the 3HFWC/AuNPs` cream. Similar results were measured by the epidermis-dermis function, where 24-28 % improvement for standard creams with AuNPs was identified, and 38.4 % for the cream 3HFWC-W/AuNPs.

ARTICLE INFO

Keywords:
Gold nanoparticles (AuNPs);
Freeze drying;
Characterisation;
Hydroxylate fullerene water complex (3HFWC-W);
Collagen;
Skin hydration;
Epidermis-dermis function;
Skin function;
Anti-ageing

**Corresponding author:*
rebeka.rudolf@um.si
(Rudolf, R.)

Article history:
Received 19 December 2021
Revised 11 February 2022
Accepted 17 February 2022

1. Introduction

Personal skin care is an important factor in slowing the appearance of age-related skin symptoms such as wrinkles, pigmented lesions, patchy hypopigmentation, actinic keratoses, thinning skin and exaggerated expression lines, all of which are a result of the internal metabolic ageing processes and external damage caused by the influx of various substances and exposure to UV light [1, 2]. Nanoparticles have recently attracted attention for use in anti-ageing cosmetics as alternatives and synergists to already established anti-ageing substances. One of the main ad-

vantages of nanoparticles is their ability to penetrate the skin barrier [3, 4], which can, potentially, result in higher effectiveness with smaller doses and shorter wear times [5]. Gold nanoparticles (AuNPs) and Hyper Harmonised Hydroxyl Modified Fullerene (3HFWC-W) have garnered special attention for use in cosmetics. AuNPs, luckily, exhibit a high degree of biocompatibility, as evidenced by their use in Cosmetics, Medical imaging and Oncology [6-8], while other metallic nanoparticles, because of their potential toxicity, represent an issue of concern when used on living organisms. The main mechanisms by which AuNPs benefit human skin are acceleration of blood circulation, anti-inflammatory properties, antiseptic properties, improving the firmness and elasticity of skin and vitalising skin metabolic processes [9-11]. 3HFWC-W is a modified form of the third allotrope of carbon – fullerene, and has been proven to offer several benefits when used on skin. The hollow one nanometre surface hydroxide functionalised spheres have increased hydro solubility, and can bond to molecules of water with hydrogen bonds [12, 13]. By establishing hydrogen bonds with the surrounding water molecules and biomolecules, 3HFWC-W improves the moisturisation and moisture retention of skin, which is considered one of the most important anti-ageing skin treatments [14].

AuNPs in suspension can be synthesised through Ultrasonic Spray Pyrolysis (USP), which has many advantages, such as the simplicity of setup and adaptability, continuous operation, relative cost-effectiveness and the possibility of easy capacity increase – i.e. scale up [15, 16]. To obtain AuNPs in dry form, freeze drying was applied for suspensions. Namely, freeze drying is the common method for the preparation of stable formulations with protein drugs, and its use and deeper understanding are becoming increasingly important from the point of view of the preparation of new, patient-friendly dosage forms in pharmaceutical products [17]. In line with the intensive increase of new temperature sensitive products, where standard drying procedure doesn't fit [18, 19], a high-quality, safe and effective nanomaterial can be provided with freeze drying.

The use of 3HFWC-W was targeted due to the fact that the combination with the nano-harmonised substance (NHS) is favourable, resulting in the functionalisation of *the* C_{60} molecule with OH groups – these processes are patented as material made from (C_{60}(OH)x) [20, 21]. The 3HFWC-W substance is based on additional water layers $C_{60}(\mathrm{OH})_{36\pm12}@(\mathrm{H_2O})_{144-2528}$. These water layers give 3HFWC-W a water liquid phase $(\mathrm{H_2O})_{144-2528}$, surrounding the solid phase—hydrogen bonded $C_{60}(\mathrm{OH})_{36\pm12}$ nanostructure. The 3HFWC-W water layers possess similar properties to liquid crystals, and they protect *the* $C_{60}(\mathrm{OH})_{36\pm12}$ complex from environmental influences, and, at the same time, they protect biomolecules from the potentially toxic effects of C_{60}. This structure, whose diameter size ranges between 6-15 nm, is a water-soluble amphiphilic biomolecule with a potential for various applications. Fullerene derivative nano-harmonised $C_{60}(\mathrm{OH})_{36\pm12}$ has shown no toxicity in tests on human dermal fibroblasts (HDF) and liver carcinoma cells [13, 22]. As a cosmetic product ingredient (its INCI name is "hydroxylated fullerene"), it could act as an active compound and a stability factor. Compared to the commercial products and vehiculums, all cosmetic products with 3HFWC-W, except body lotion, have shown significant improvements of the functionality of the basement membrane [23]. While regenerating cream and body lotion with 3HFWC-W have positively affected collagen quality in the dermis, anti-ageing and hand cream with 3HFWC-W have shown positive effects on signal transduction and regeneration of collagen. Results imply that anti-ageing and hand cream with 3HFWC-W, as well as body lotion vehiculum, could improve the properties of the basement membrane and accelerate signal transduction in the dermis, and, finally, enable faster regeneration of the epidermis and rapid reaction of the skin to negative environmental influences [23]. Regenerating cream with 3HFWC-W has shown positive effects on the basement membrane and strength of the collagen supportive structure in the skin. The body lotion with 3HFWC-W and commercial hand cream have improved the mechanical properties of the skin through strengthening collagen fibres in the dermis. The ingredient 3HFWC-W, which acts in a natural, biophysical way on the skin, might open a new era in the way we understand and treat changes in the altered and ageing skin. Depending on the type of cream, the average improvement was 22.5 %, based on the arithmetic value of 12 % (body lotion), 18 % (regenerating cream), 28 % (anti-ageing), and 32 % (hand cream). Based on the presented clinical studies and results, in order to achieve an even

more visible anti-ageing effect, it was hypothesised that an additional effect could be achieved with AuNPs that are highly biocompatible and have some baseline functional properties [24, 25].

The focus in this dermatological study was, therefore, to find the effect of AuNPs not only in cosmetic standard creams, but also in combination with 3HFWC-W, to get a potentially new complex in cosmetics. In the first step creams were prepared, followed by six weeks of testing on volunteers. In order to evaluate the activity of the AuNPs in creams, characterisation of the cream`s ingredients was performed, and real-time analysis of the skin anti-ageing effect was done on the volunteers.

2. Materials and methods

2.1 Materials

The starting materials for the preparation of AuNPs` suspensions were two precursors: Au chloride salt – (gold (III) chloride tetrahydrate – trace metals basis 99.9 %, Acros Organics, Germany) and Au acetate salt – (gold (III) acetate, Alfa Aesar, USA). Collection mediums were prepared with D.I. water and two steric stabilisers: Polyvinylpyrrolidone (PVP40 Sigma Aldrich, Germany) and polyethylene glycol (PEG 6000, Fisher Scientific, UK). Other chemicals were: Sodium hydroxide (NaOH, Fisher Chemicals, Germany) and hydrochloric acid (HCl, 37 %, Sigma Aldrich, Germany). Three types of AuNPs` suspensions were prepared for cosmetic creams with the characteristics shown in Table 1 (these names/abbreviations are used throughout the text). Preparation of the 3HFWC-W took place under controlled conditions. The first step was water purification from tap water to water with 0.1 μS/m conductivity. The main ingredient, fullerol $C_{60}(OH)_{36}$ with purity of 99.99 %, was imported from Solaris Chem in Canada. A specified amount of fullerol was mixed with the purified water in a vessel at temperatures of 33-400 °C. After achieving a satisfying solubility the solution was transferred to another vessel, where it was exposed to an oscillatory magnetic field of 100-250 mT in order to create aqueous layers based on strong hydrogen bonds [20, 21]. The result was 3HFWC-W: $C_{60}(OH)_{36}@(H_2O)_n^l$, size of 6-15 nm, with *n*-water molecules (600-200) and *l*-water layers (1-6). 3HFWC-W was mixed in a concentration of 18 % by a standard procedure with 34 % of aqua purificata and 48 % of standard cream base (TFT Nano Center, Belgrade, Serbia).

Table 1 Characteristics for all three types of AuNPs` suspensions

AuNPs` suspension	Type of Stabiliser – concentration in D.I. water (g/L)
AuNC PEG10	PEG – 10 g/L
AuNC PVP5	PVP – 5 g/L
AuNA PEG20	PEG – 20 g/L

Table 2 Composition of 3HFWC-$W^{Au\ NP\ PEG\ 20}$ cream

Formula	Product identifier	Quantity (wt. %)
$C_{60}(OH)_{36\text{-}48}@\ (H_2O)_{950\text{-}2100}$	3HFWC-W	18.00
AuNPs	AuNPs (AuNA+PEG 20 g/L)	0.05
H_2O	Ultra-pure water (0.055 μS/cm)	32.95
AB	Ambiphilic base	49.00
3HFWC-$W^{AuNP\ PEG20}$	Nano gold hyperharmonized fullerene water complex	100.00

2.2 Methods

Synthesis of AuNPs` suspensions

AuNPs` synthesis was done on a custom built USP device, located in Zlatarna Celje d.o.o., Slovenia. The device was constructed from a custom aerosol generator based on a 1.6 MHz piezoelectric transducer (Liquifog II, Johnson Matthey Piezo Products GmbH, Germany), which aerosolises the Au precursor solution. The aerosol droplets were transferred by a constant flow of carrier gas (N_2) into a heated multi zone reactor tube made from quartz glass. The first zone facilitates the evaporation of the aerosol droplets and the formation of a solid aerosol. In the second reaction zone the temperature is increased to initiate thermal decomposition in the presence of a

reducing gas (H_2) and continues with the reduction of Au^{+3} into elemental Au^0. The final zone facilitates the sintering of AuNPs, which are finally collected in a system composed of three connected gas wash bottles. The collection medium was with D.I. water, with PVP, or PEG at different concentrations. The detailed parameters of the AuNPs` synthesis and USP device are the subject of a patent for AuNPs` production [26]. The synthesised AuNPs` suspensions are marked AuNC when a chloride precursor was used, and as AuNA in the case of the acetate precursor. The starting concentration of [Au] in all the prepared precursors was 0,5 g/L. The technological USP parameters, such as temperature profiles, gas flows, were also consistent with previous experimental trials [27, 28].

Freeze drying of AuNPs` suspensions

A separation process was applied for AuNPs` suspensions in order to obtain AuNPs in dry form (Fig. 1). As the removal of the liquid phase from the AuNPs` suspensions must be done in a way to retain the AuNPs` size distribution and to keep their properties, they cannot be separated using mechanical processes. Based on this, the use of a thermal process was proposed in the form of freeze drying. In the case of freeze drying, the advantages over other forms of drying methods are in: (i) Preserving the structure, shape, and size of the AuNPs, (ii) Extending the life span of AuNPs, (iii) Rehydration of dry AuNPs is possible, (iv) The sample is placed directly into the container, which can be sealed in-situ in the freeze drier, thus avoiding potential contamination. The idea of the freeze drying process was in freezing the AuNPs` suspension, therefore stabilising the AuNPs` size distribution, which was followed by a rapid decrease of the system pressure to a few Pa, causing sublimation of the carrier liquid phase. In this way, when the frozen liquid was sublimated, all that remained was the AuNPs`/stabiliser powder inside the container. The intensity of the process was controlled by the temperature of the heating shelves and system pressure. Since the synthesis of AuNPs with USP and subsequent freeze drying process for producing dried AuNPs is not yet readily available in literature or otherwise [29], the selection of system pressure and shelf temperature that led to a stable, yet reasonably fast process (allowing the removal of the liquid without AuNPs` entrainment from the process of the drying protocol), had to be aligned to get stable process behaviour. In the case of 3HFWC-W products for cosmetics, the AuNPs` suspension was dried in a Miron glass cosmetic jar, which was later also used as the final cosmetic product envelope.

Freeze drying was performed in a laboratory freeze dryer manufactured by Kambic (LIO 2000LFT, Slovenia). The dryer had a separate drying chamber with two temperature regulated stainless steel shelves, each with a shelf area of about 0.09 m^2, and a condensation chamber with a condenser capacity of 5 kg. The shelf temperature during the freeze drying can be varied between –40 °C and 40 °C, and the temperature of the condenser can be set to –90 °C. The chamber pressure was measured with a Pirani gauge, which was also used to regulate the vacuum pump (see Fig. 1).

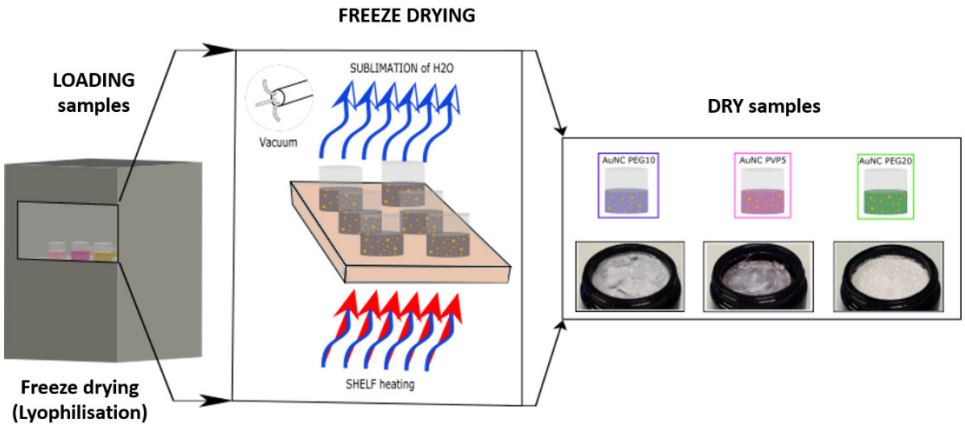

Fig. 1 Prepared and freeze dried AuNPs: AuNC PEG10, AuNC PVP5 and AuNA PEG20

In the drying cycles, 30 Miron glass cosmetic jars were filled with 80 ml of AuNPs` suspensions and placed on the temperature regulated shelves. After filling, every jar was weighed and placed in its corresponding position. To limit the heat gains from the surroundings, arising due to the front plexiglass observation doors, the front door was covered with a styrodure plate enveloped in aluminium foil. To limit the effect of the ice build-up on the condenser surfaces, the condenser was defrosted completely before each drying run. The freezing phase lasted for 15 hours at the shelf temperature –40 °C and atmospheric pressure. This was followed by the primary drying phase at the shelf temperature of –20 °C and the chamber pressure of 12 Pa for 67 h. This was followed by the secondary drying at the same pressure, and shelf temperature of 10 °C for the next 40 hours. The key parameter in the freeze drying phase was to adjust the heat release from the tray to samples during the primary drying phase according to the pressure level in the vacuuming phase, and not to collapse the samples.

Preparation of creams with AuNPs and 3HFWC-W

Creams with dried AuNPs (AuNC PEG10, AuNC PVP5 and AuNA PEG20) were obtained according to the procedure for the preparation of cosmetic creams, by mixing AuNPs in the weight percentage of 12 %, aqua purificata 48 % and standard cream base 40 % [30]. The 3HFWC-W$^{AuNA\ PEG20}$ cream was obtained by mixing 18 % 3HFWC-W, 0.05 % AuNA PEG20, 32.95 % aqua purificata and 49 % ambiphilic base (standard cream base).

AuNA PEG20 were chosen to be mixed with the 3HFWC-W substance in the ratio 1:10, giving a 3HFWC-W$^{AuNA\ PEG20}$ complex (Fig. 2). A commercial base ("U", Unichem Pharm) was used, without any active ingredient. In weight, pure water (0.1 μS/cm) was 35 %, the base "U" 45 % and the active ingredient 3HFWC-W$^{AuNA\ PEG20}$ was 20 %. The creams were prepared by a standard procedure using a mixing machine, the Unguator E/S (Gako International), which is individually programmable. The jar size was 500/600 ml (rated volume/filling volume).

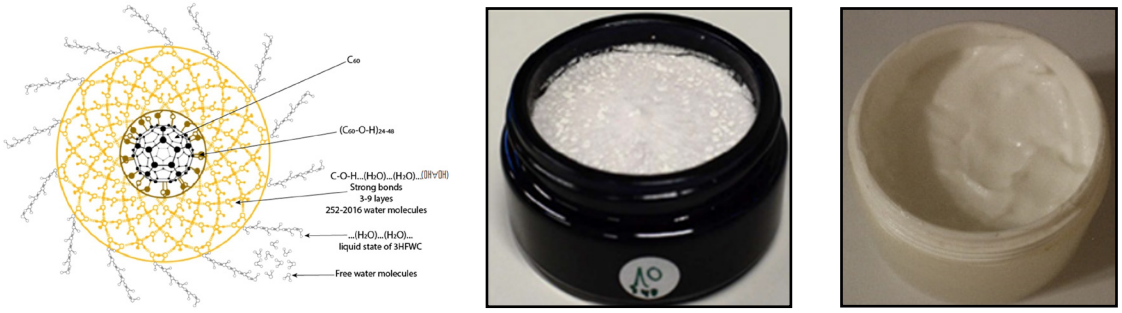

a) b) c)

Fig. 2 Schematic presentation of the cream components and cream: a) 3HFWC-W substance, b) Dried AuNA PEG20, and c) 3HFWC-W$^{AuNA\ PEG20}$ cream

2.3 Characterisation methods

Inductively Coupled Plasma-Mass Spectrometry (ICP-MS)

The concentration of Au in the synthesised AuNPs` suspensions for all three types was measured with Inductively Coupled Plasma-Mass Spectrometry (ICP-MS). The spectrometer used was an HP, Agilent 7500 CE, equipped with a collision cell (Santa Clara, CA, USA). The following conditions were used for the ICP-MS: The power was 1.5 kW, Nebuliser-Meinhard, plasma gas flow was 15 L/min, nebuliser gas flow was 0.85 L/min, make up gas flow was 0.28 L/min and reaction gas flow was 4.0 mL/min. The instrument was calibrated with matrix matched calibration solutions. The relative measurement uncertainty was estimated as ±3 %.

Dynamic Light Scattering (DLS) and measurements of ζ potential

DLS measurements of the hydrodynamic size distribution of AuNPs in aqueous suspension and measurements of ζ potential were performed with a Malvern Zetasizer Nano ZS (Malvern Panalytical, Worcestershire, UK). The hydrodynamic size distribution of AuNPs was measured using disposable plastic cuvettes and ζ potential measurements were done using a closed capillary cell

with electrodes. DLS and ζ potential measurements were performed with the following parameters for AuNP suspensions: Refractive Index (RI) = 0.2, absorption = 3.32; the suspension properties were: Dispersant = water, Refractive Index (RI) = 1.33, viscosity = 0.887 cP, temperature = 25 °C, equilibration time = 30 s, angle of incidence = 173° backscatter, dielectric constant = 78.5. Measurements were performed in 10 series at a time of 10 s per series, and the measurement was repeated 3 times.

Scanning Electron Microscopy (SEM)

A Scanning Electron Microscope, Sirion 400NC (FEI, USA), with an Energy-Dispersive X-ray spectroscope (EDS) INCA 350 (Oxford Instruments, UK), was used for the SEM analysis. The AuNPs` suspensions were put dropwise onto the SEM holders (mesh) with conductive carbon adhesive tape, which allowed better SEM observation. The SEM holders were left to dry in a desiccator for one day before the SEM investigations were carried out. The dried AuNPs were placed directly on conductive carbon adhesive tapes and observed as is.

Transmission Electron Microscopy (TEM)

A JEOL 2100 (JEOL, Japan) and JEOL JEM-2200FS HR (JEOL, Japan), operating at 200 kV, were used for the TEM observations of the cream with AuNPs. All of the samples were first dispersed in ethanol, and then a drop of each of these samples was put on a copper TEM grid with an amorphous carbon film. The grids were then dried before they were used for the TEM investigations.

Opto-Magnetic Imaging Spectroscopy (OMIS)

The effects of the creams with AuNPs were examined using Opto-Magnetic Imaging Spectroscopy (OMIS), a diagnostic method which is based on light-matter interaction, and has been applied to characterise water and skin layers [31, 32], cervical cancer and colon cancer [33], [34], collagen and skin miniaturisation [2, 23]. The OMIS detects reflected diffuse and polarised white light after their interaction with tissue, since the energy of photons of visible light (1.6- 3.0 eV) is the same value as valance electrons. The method of examination is its ability to detect paired (p^-) and unpaired (p^+) electrons as the paramagnetic and diamagnetic properties of the specimen.

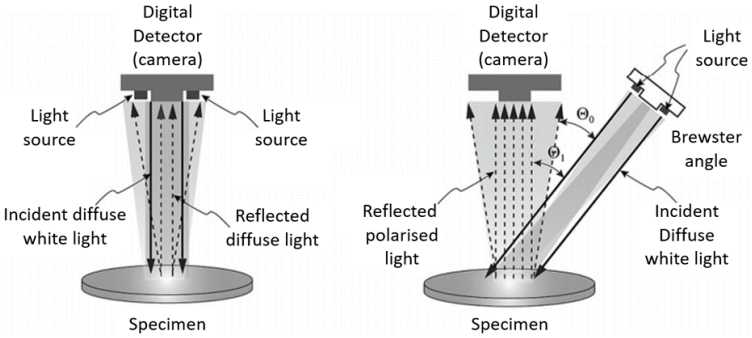

Fig. 3 Schematic representation of the Opto OMIS method [35]

As shown in Fig. 3, the device consists of two light sources, which emit the same light, one at an angle of 90° and the other at an angle of 53° (Brewster angle for the skin) to the sample, and a detector (camera) to collect the reflected light. There are two different types of light after the interaction with the tissue – one being reflected as diffuse (the one coming from the source at a right angle), and one being reflected as polarised (coming from the source at the Brewster angle). When reaching the detector, polarised light contains only its electrical properties, while diffused light contains both magnetic and electrical properties. By subtracting these two lights, the magnetic component is able to determine the paramagnetic and diamagnetic properties of various layers of the tissue of interest. The light source contains light-emitting diodes (LEDs) of different wavelengths (ultraviolet, green, red, infrared and white), and the detector collects the reflected light using three channels: Red, green and blue (all contained in white light). Since

those wavelengths go through skin to different depths (as shown in Fig. 4), it's possible to determine the biophysical properties of its layers. The biophysical skin properties (diamagnetic/paramagnetic) were measured using OMIS as an innovative patented diagnostic method [36]. Fig. 4 shows the second-harmonic function, which is a nonlinear optical process, where two photons with the same frequency interacting with a nonlinear material, are "combined", and generate a new photon with half the wavelength and twice the frequency of the photons, which can serve the coherence of the excitation. It means in the skin, as nonlinear media, a UV photon of 390 nm (omega) will generate as two photons of 780 nm (2 × 390 = 780 nm) and penetrate deeply into the skin. Also, the process could be inversion, two photons of 780 nm may generate a photon of 390 nm if they activate certain nonlinear media.

In the analysis method, Higuchi Fractal Dimension (HFD) was used as one of the parameters for analysis. The Higuchi algorithm is a technique for calculating the fractal dimension of a time series. The usage of the Higuchi method leads to very precise values of the fractal dimension and shows the complexity of the time series studied. HFD is fast, and applicable in real-time calculations. Contrary to the linear methods, HFD can be applied directly to nonlinear time series, and it is suitable for short time series` analysis. HFD needs to be provided with only one input parameter, specifying the maximal distance between the points compared in the time series [38, 39].

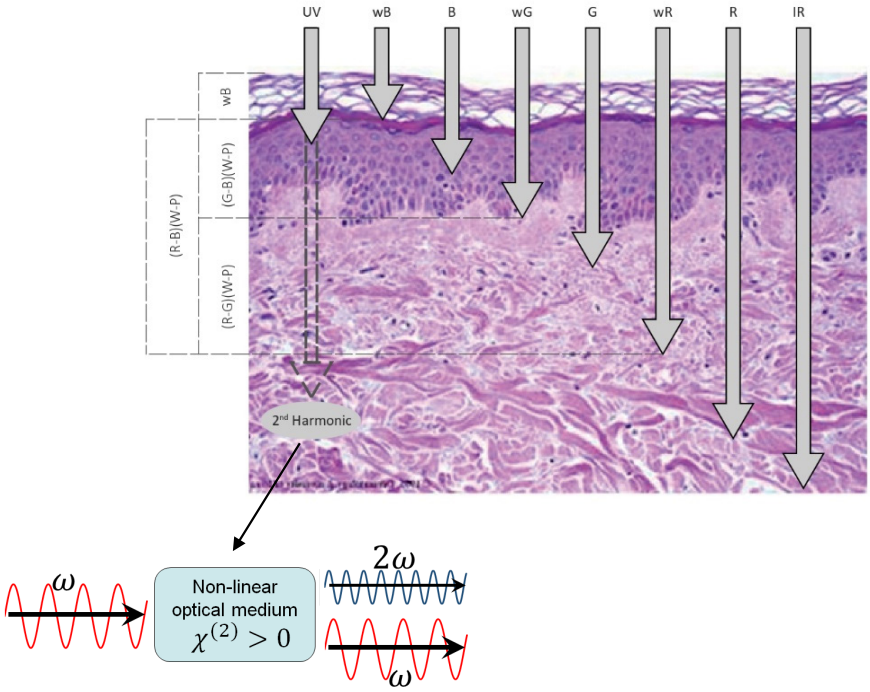

Fig. 4 Skin cross-section and penetration of light of different wavelengths (from UV to IR) (wB – Blue channel of white LED light, B – Blue LED light, wG – Green chanel of white LED light, G – Green LED light, wR – Red channel of white LED light, R – red LED light, (G-B)(W-P) - Green minus Blue channel of white LED light (diffuse) and white polarised, (R-G)(W-P) Red minus Green channel of white LED light (diffuse) and white polarised, (R-B)(W-P) Red minus Blue channel of white LED light (diffuse) and white polarised) [37]

Volunteers` testing

A six-week study was conducted to examine the effects of AuNPs and 3HFWC-W in new creams, as well as their synergistic effects. The volunteers were 33 women with an average age of 37 years, with the oldest participant being 65 and the youngest 21 years old, and they were divided into four groups. Every volunteer was given two cream samples and instructions to apply them twice a day on their forearm. One cream was the base of the standard cream without AuNPs (as control), which was the same for all four groups. Three groups tested creams with a standard base and with AuNPs, while the fourth group tested cream with the new complex AuNPs and 3HFWC-W. During the study two areas on the volunteers` forearms were filmed every seven days. After six weeks we had usable data for 33 volunteers.

3. Results and discussions

3.1 ICP-MS

To ensure consistency between the differently stabilised AuNPs, the Au content of the initial suspensions with ICP-MS was determined, and they were diluted with the appropriate amount of D.I. water. The final measured concentrations of Au in all the prepared AuNPs` suspensions are shown in Table 3.

Table 3 Au concentration in the prepared AuNPs` suspensions

Au suspension	Au concentration (ppm)
AuNC PEG10	120
AuNC PVP5	150
AuNA PEG20	100

3.2 DLS measurements

The principle of size measurement is based on Rayleigh scattering resulting from the Brownian motion of AuNPs whose size is less than the wavelength of the incident light at a fixed scattering angle [40]. The reason for choosing this technique for size distribution was the spherical shape of the AuNPs, which was confirmed by the pronounced colour of all the obtained suspensions. To determine the mean size distribution of AuNPs, DLS measurements were performed on all three suspensions with the presence of the selected stabilisers. The estimated Z-average AuNPs in the AuNC PEG10 suspension was 146.9 nm, in AuNC PVP5 190.9 nm and in AuNA PEG20 342.3 nm. The histogram data for the PDI index and the shape of the size distribution curve are shown in Fig. 5. The curves show a slight difference between the mean hydrodynamic radius of AuNPs in the AuNC suspensions produced from the same AuNC precursor. This difference was most likely caused by the difference between the PEG and PVP stabilisers. AuNPs prepared from the organic AuNA precursor were, on average, much larger than the AuNPs prepared from the inorganic AuNC precursor. The DLS measurements demonstrated somewhat larger AuNPs sizes than expected, while SEM and TEM observations show much smaller sizes of primary AuNPs in groups, and soft agglomerates in the PVP and PEG medium. Soft agglomerate AuNPs are held together by weak, physical van der Waals forces, while hard agglomerates (or aggregates) are usually nanoparticles with stronger chemical or sintering bonds between them [41, 42]. It is difficult to discern between primary nanoparticles and agglomerates with optical mobility measuring techniques [43], such as DLS. The agitation and light mechanical force applied during mixing of the AuNPs in the creams confirmed the presence of soft agglomerates, as they were disrupted into individual AuNPs, seen in the investigations of the prepared creams shown below.

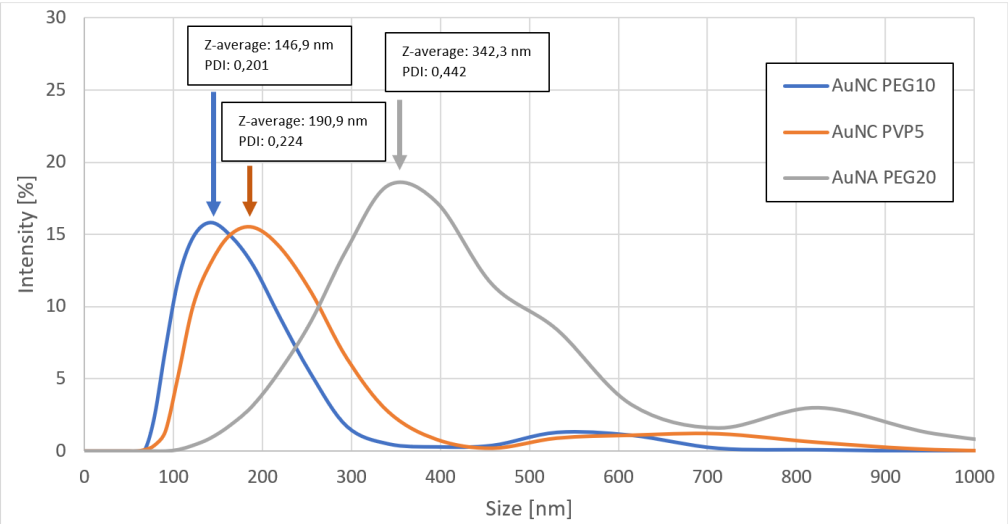

Fig. 5 DLS size distribution of AuNPs in suspensions: AuNC PEG10, AuNC PVP5 and AuNA PEG20

3.3 ζ potential

AuNPs in a suspension of D.I. water synthesised with USP exhibited a slight negative surface charge that was not significant enough to prevent agglomeration. Therefore, the addition of steric stabilisers was needed to ensure a stable suspension. This was achieved with the addition of water-soluble polymers such as PEG or PVP, that physically prevent the AuNPs from coming in close contact with each other, without having a significant effect on the surface charge of the AuNPs. The measured ζ potential of the stabilised AuNPs suspensions is shown in Table 4. Significantly, PVP had the most negative charge. It is a well-established phenomenon that PVP has the ability to reduce the surface charge of AuNPs [44 -46].

Table 4 Results of ζ potential for all AuNPs` suspensions

AuNPs` suspension	Type of Stabiliser concentration in D.I. water [g/L]	ζ potential
AuNC PEG10	PEG – 10 g/L	-1.56 ±8.15 mV
AuNC PVP5	PVP – 5 g/L	-3.12 ±4.66 mV
AuNA PEG20	PEG – 20 g/L	-1.53 ±8.21 mV

3.4 SEM observations

AuNPs in all three suspensions were spherical in shape (see Fig. 6). The average sizes of the smaller AuNPs ranged from 74 nm to about 95 nm. The presence of bigger AuNPs was also confirmed, in the range of about a couple of hundred nanometres. These represent a group of soft agglomerates that are easily dispersed during the redispersion process. Hard agglomerates of connected primary AuNPs were not detected in this study. Several point EDS analyses were performed on the surface of AuNPs to confirm the purity and content of Au. The obtained results showed a high purity of Au, especially for the case of nanoparticles from AuNA (96.10 wt. %). The rest represents O, the origin of which can be attributed to bonds with the stabiliser. No other impurities were detected.

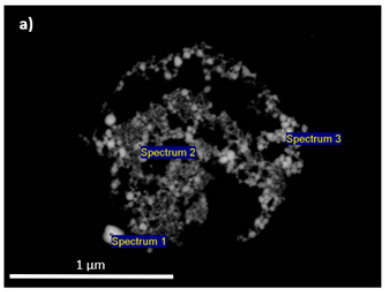

Spectrum	O	Au
Spectrum 1	6.73	93.27
Spectrum 2	22.81	77.19
Spectrum 3	16.29	83.71
Mean	15.27	84.73
Std. deviation	8.09	8.09
Max.	22.81	93.27
Min.	6.73	77.19

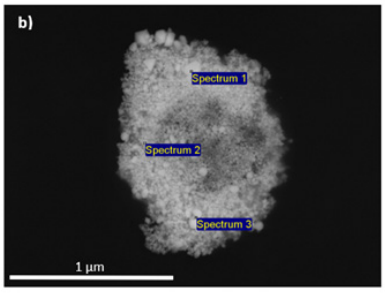

Spectrum	O	Au
Spectrum 1	5.13	94.87
Spectrum 2	8.07	91.93
Spectrum 3	7.03	92.97
Mean	6.74	93.26
Std. deviation	1.49	1.49
Max.	8.07	94.87
Min.	5.13	91.93

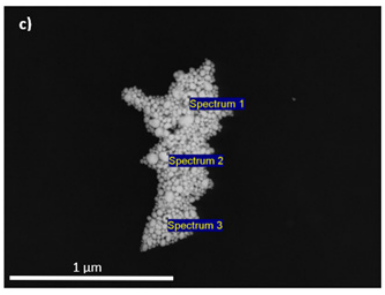

Spectrum	O	Au
Spectrum 1	3.71	96.29
Spectrum 2	3.67	96.33
Spectrum 3	4.32	95.68
Mean	3.90	96.10
Std. deviation	0.37	0.37
Max.	4.32	96.33
Min.	3.67	95.68

Fig. 6 SEM micrographs and results of EDS point analyses in wt. % for AuNPs: a) AuNC PEG10, b) AuNC PVP5 and c) AuNA PEG20

The chemical composition of the synthesised AuNPs was checked by EDS (see Fig. 6), and the results have shown the presence of a high gold content (more than 85 wt. %) with oxygen originating from the stabilisers (PEG or PVP) at individual sites of the surface AuNPs.

3.5 Circularity and size of AuNPs

The calculated average circularity was 0.9 for all tested AuNPs (with a 0-1 range, 0 signifies an irregular shape and 1 signifies a perfect circle). Table 5 shows the experimentally measured mean AuNPs sizes compared to the theoretically calculated values, which were calculated based on data from literature [47]. There was a difference between the theoretically calculated and experimentally obtained sizes of synthesised AuNPs, which were bigger and not finely dispersed. The synthesised AuNPs had a mixture of different morphologies, which was not taken into account in the theoretical calculations. The aerosol droplets were also generated in a size distribution, rather than a single droplet size. The coalescence of aerosol droplets was also not considered, which is difficult to prevent, as the gas flows in an enclosed system where turbulence effects are to be expected. The microporosity of the AuNPs was not seen after synthesis, the result of which would perhaps be an even greater discrepancy between the experimental and theoretical values. It was observed from the SEM measurements that the AuNPs in suspensions had almost a unimodal size distribution. Namely, the AuNPs in AuNC PEG10 had an average size with a peak at 84.94 nm (in the range 20-100 nm there were 88 % of the total AuNPs), the AuNPs in AuNC PVP5 had an average size with a peak at 97.39 nm (in the range 20-100 nm there were 92 % of the total AuNPs) and AuNPs in AuNA PEG20 had an average size distribution with a peak at 104.25 nm (in the range 20-100 nm there were 93 % of the total AuNPs). The results are not completely consistent with the SEM micrographs, as the SEM images should be considered to show slightly higher AuNPs, due to insufficient high resolution and charge build-up due to stabiliser residues.

Table 5 Experimentally measured average AuNPs` size compared to the theoretically calculated values

Au suspension	Average size of synthesised AuNPs (nm)	Theoretically calculated AuNPs` size (nm)
AuNC PEG10	74.94	94.53
AuNC PVP5	87.39	94.53
AuNA PEG20	94.25	91.55

3.6 TEM observations

The prepared cosmetic creams were observed with TEM to determine how AuNPs were incorporated into the matrix of the base cream. As can be seen in the obtained TEM images (Fig. 7), the AuNPs were quite well integrated with the other components of the base cream, which is the basic requirement for cosmetics` application. The monodispersity and stability of the different AuNPs was achieved and is shown by the red circles in the TEM images for each test cream separately. A more detailed investigation showed that there was no agglomeration of AuNPs, and that they were mixed well with the base substance of the cream.

TEM investigations were also carried out for the cream 3HFWC-W/AuNPs, Fig. 8. Fullerene from 3HFWC-W was found to be in direct contact with the smaller AuNPs (visible with a red arrow). The size of the this fullerene was around 10 nm with completely spherical shapes, which is consistent with the TEM photographs obtained by other authors [48, 49].

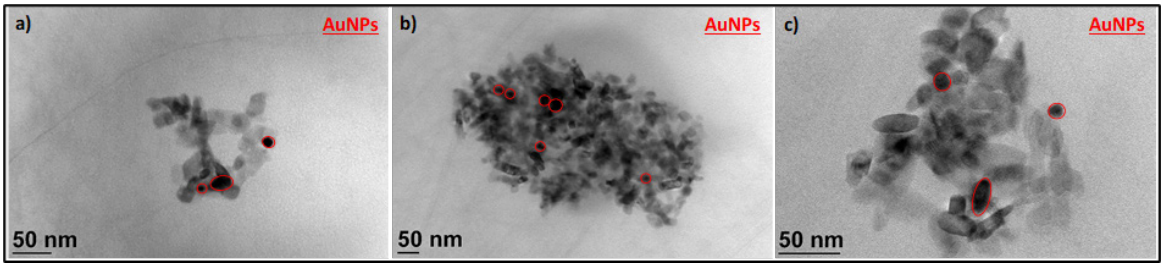

Fig. 7 TEM micrographs of AuNPs taken from cosmetic creams with: a) AuNC PEG10, b) AuNC PVP5 and c) AuNA PEG20

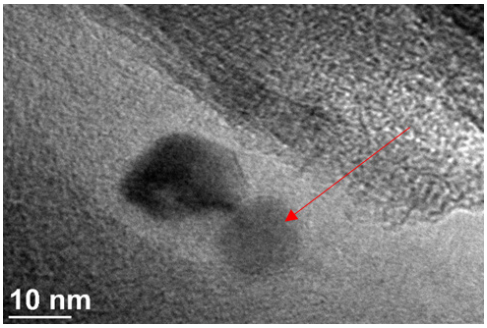

Fig. 8 TEM micrographs of fullerene from 3HFWC-W (red arrow) in contact with AuNPs

3.7 Cream test results

Predispositions and limitations in this study were: In order to obtain information about the epidermis, we had to subtract the values obtained on the blue channel from the values of the reflected light obtained on the green light channel, and, thus, we obtained the w(G-B) convolution of the spectrum. As seen in Fig. 4 wG penetrates to the bottom of the epidermis and wB to the dream stratum corneum, so the w(G-B) convolution gives us complete information about the biophysical characteristics of the epidermis.

In the attached graph of Fig. 9, which represents the average values of all participants, it can be seen that there was a shift in the peak as well as a change in its intensity. The obtained values give us information on the number of paired (p+) and unpaired electrons (p-), i.e. on the paramagnetic and diamagnetic characteristics of the skin.

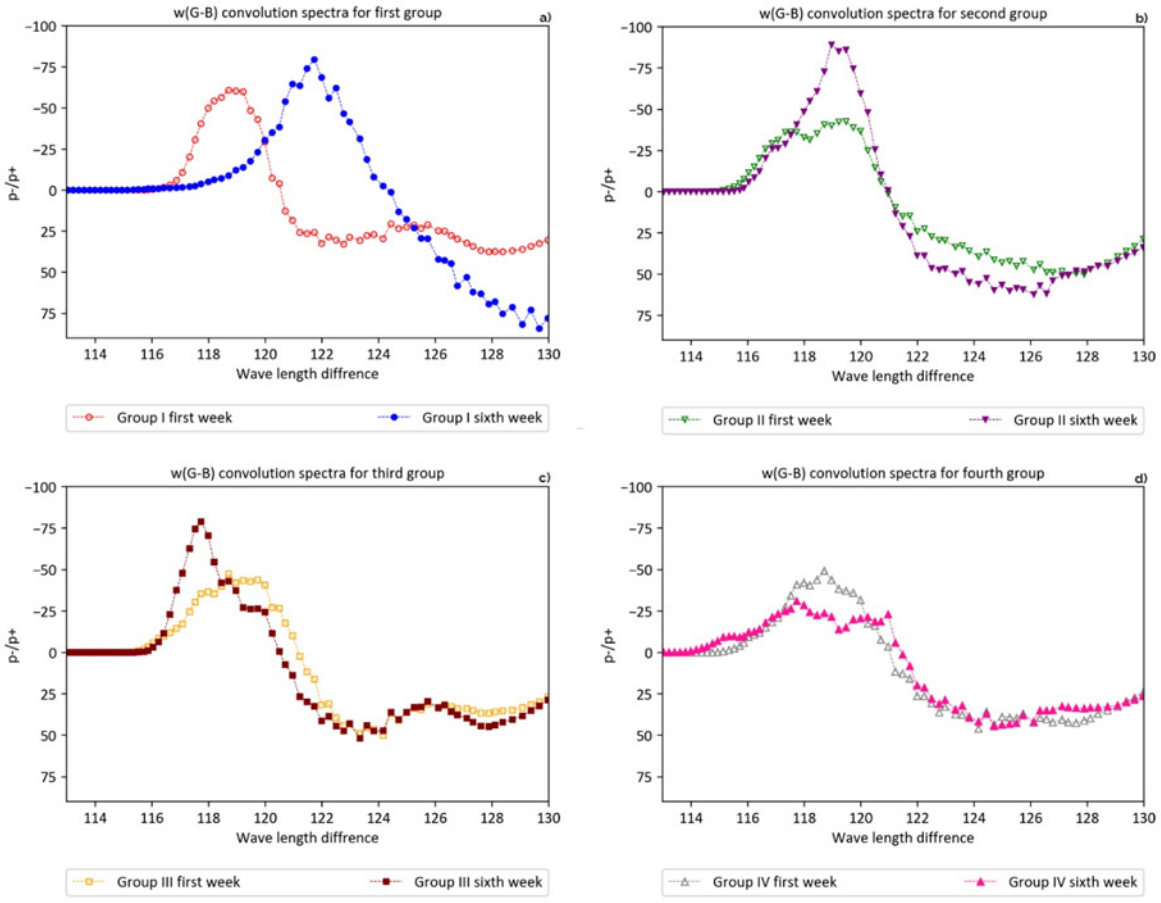

Fig. 9 Change of (p-/p+) electrons in the epidermis before and after using creams with a) AuNC PEG 10, b) AuNC PVP5, c) AuNA PEG20 and d) 3HFWC-W$^{AuNA\ PEG20}$

In Fig. 9a the change in the number of (p-/p+) electrons in the epidermis is visible for a group of participants who used a cream with AuNC PEG 10. In the case of AuNC PVP5 cream, according to the attached graph (Fig. 9b), it can be noticed that there was a change in the intensity of the peak, but not its shifting, which is a possible consequence of the surface energy of AuNPs interacting with the skin [50]. Since these are larger AuNPs compared to the first group, their surface energy is lower. In the values obtained by averaging the data on the biophysical state of the skin, volunteers of the third group, cream with AuNA PEG20, we noticed an even smaller change in the intensity of the peak because their surface energy was the lowest (Fig. 9c). Cream with 3HFWC-W$^{\text{AuNA PEG20}}$ used by the volunteers of the fourth group represents a symbiosis of AuNPs and 3HFWC-W substances. AuNPs have a negative surface energy [51], which is why hydrogen atoms from aqueous layers in 3HFWC-W are oriented towards them, thus creating a coating around the AuNPs ($2r$ < 95 nm). Thanks to this homogeneous structure, the substance neutralises the negative charge of AuNPs, which is why the changes in the intensity of the peak were the smallest in this group (Fig. 9d).

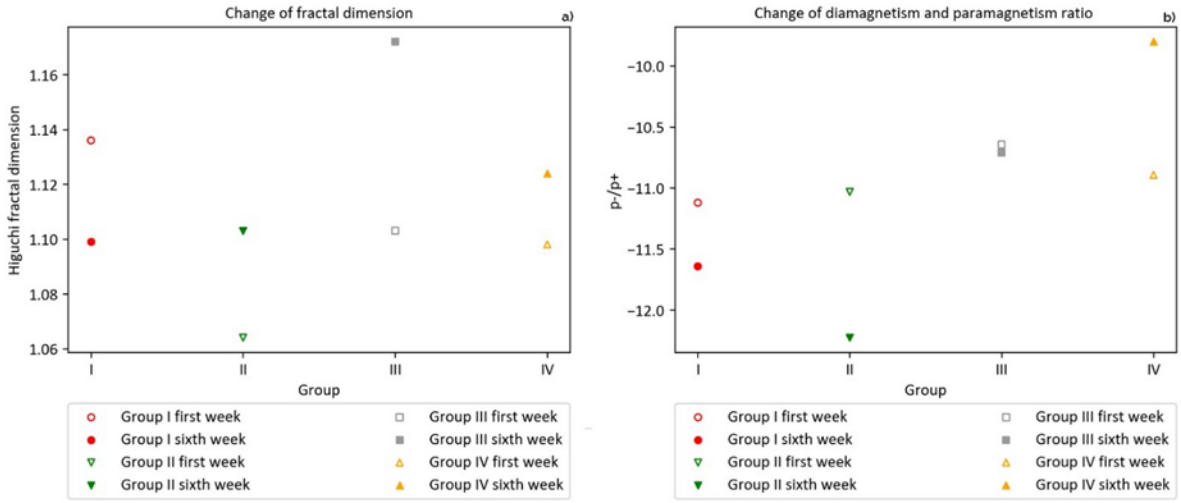

Fig. 10 Diagram of Higuchi fractal dimension (HFD) as one of biophysical parameters of epidermis properties-HFD gives the dynamics of (p^-/p^+) electrons tissue: a) for all four groups before and after six weeks treatment for different types of light. b) Diagram of the average biophysical properties of the epidermis (p^-/p^+) electrons for all four groups before and after six weeks of treatment for different types of light

The fractal dimension (see Fig. 10a) of the graph for the first week of the third group is D_f = 1.417, while for the sixth week D_f = 1.5, which indicates that there has been a change in the dermis. The change is different with the fourth group, since the fractal dimension for the first week is D_f = 1.346, and for the sixth D_f = 1.235. When other parameters are taken into consideration, such as the ratio of (p+/p-) electrons, then we see that for group III, for the first week the result equals -95.38, and for the sixth week -96.67, which indicates that the cream with AuNPs did not affect the fibroblasts and collagen synthesis significantly, which is in accordance with the increase in fractal dimension by 6.3 % in group III subjects. In group IV, which for the first week had approximately the same value (p+/p-) = -95.65 as in group III (-95.38), while in the sixth week there was a significant change in collagen synthesis in group IV subjects. The change of diamagnetism and paramagnetism ratio presented in Fig. 10b as value (p+/p) increased significantly for group IV, the change in the sixth week compared to the first was even 73.7 % better. This is in accordance with the change in the fractal dimension of the signal obtained from the dermis because the fractal dimension of the signal spectrum decreased by 8.6 % due to the balanced dynamics of the oscillatory processes in the depth of the dermis, where collagen is dominant.

Next, if we look at the results in Table 6, where the change of biophysical properties of skin for dermis are presented according to the data for red light depending on the difference in wavelength (nm), intensity (n. a. u.), surface ratio (p+/p-) and fractal dimensions, the following findings can be made. In previous studies with a cream containing only the 3HFWC-W substance

(without AuNPs), an improvement in effect by 28 % was achieved, what is comparable to other creams that had the same base as classic bioactive ingredients. When AuNPs with 3HFWC-W were combined in cream, significantly better improvement was achieved by 73.7 % (a difference of 45.7 %), which is an obvious beneficial effect of the new cream. This can be attributed to the result of the new combination of nano-quantum substance and functional properties of AuNPs (AuNPs@3HFWC-W).

Table 6 Change of biophysical properties of skin for dermis according to data of red (R) light for all four groups: 1. (AuNC PEG 10), 2. (AuNC PVP5), 3. (AuNPsPEG20) and group 4. (3HFWC-W$^{AuNA\ PEG20}$)

Light	Week	Unit	1. Group		2. Group		3. Group		4. Group	
			D	P	D	P	D	P	D	P
W (G-B)	1	Int (n.a.u)	-60.85	37.57	-42.62	50.67	-47.48	49.92	-49.38	45.87
		WLD (nm)	118.71	128.37	119.48	127.33	118.71	124.16	118.71	124.16
		(p+/p-)	-11.12		-11.03		-10.64		-10.89	
		D_f	1.136		1.064		1.103		1.098	
	6	Int (n.a.u)	-79.52	84.19	-89.21	62.25	-78.92	51.70	-31.13	44.52
		WLD (nm)	121.73	129.669	118.97	126.10	117.79	123.34	117.73	124.71
		(p+/p-)	-11.64		-12.23		-10.71		-9.80	
		D_f	1.099		1.103		1.172		1.124	

4 Discussion

The perception of gold as an inert material was altered by the discovery that AuNPs are chemically reactive. Their properties can be adapted to certain applications by controlling the size and atomic structure on the surface of the AuNPs. Suspensions with different stabilisers such as PEG and PVP were used during the drying of AuNPs` suspensions with lyophilisation in a laboratory lyophiliser. At the same drying conditions in miron glass cosmetic jars, the dried material with PVP was more stable and no entrainment of dried material was noted, where, on the other hand, with the use of PEG stabiliser, the dried cake was more sensitive to sublimated solvent vapour, which always entrained some fraction of the dried material out of the miron glass cosmetic jars. The use of PVP in cosmetics` application is also beneficial, and exhibits the best performance in binding capacity, solubility, film formation and emulsifying performance [52]. The reduction in surface charge mediated by PVP allows for more positively charged 3HFWC-W to be coordinated around the surface of the AuNPs [44-46]. This allows for an increased transfer of -OH ions.

The proposed binding mechanism between AuNPs and 3HFWC-W is mediated by the stabilising polymers. Specifically, by the oxygen and nitrogen atoms that are present in their macromolecular chains. Here, oxygen and nitrogen atoms act as electron donors to the almost 0 surface charge of the AuNPs [53]. This interaction allows for weak surface binding of the polymers to the surface of the AuNPs [44, 45]. Due to the inherent charge of the polymers being negative, this, in turn, allows for electrostatic attraction between the AuNPs and the polymer stabiliser complex, to attract and coordinate 3HFWC-W around its hydrodynamic radius. Zeta potential measurements suggest that PVP offers more binding locations in comparison to PEG if one looks at the molecular conformation of PVP and PEG, as shown in Fig. 11, with the proposed binding. In PEG the oxygen atoms that interact with AuNPs and 3HFWC-W are in the main macromolecular chain, while, in comparison, the interacting oxygen and nitrogen in PVP are a side functional group. This steric and functional difference most likely enables a closer interaction between the AuNPs` surface and the molecule, causing a higher binding energy. One must also note that the monomer unit (marked by square brackets) of PVP offers two binding points when compared to the one of PEG. Since this coordinated complex is formed in a solution of water and stabiliser, we presume that, due to the creams being emulsions containing a separate aqueous and lipoic phase, that the complex is stable in the aqueous phase.

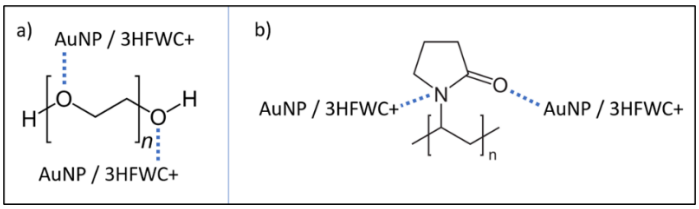

Fig. 11 Presentation of a binding scheme of AuNPs or 3HFWC-W with a) PEG and b) PVP. As there are hydrogen atoms on the surface of the AuNPs or 3HFWC-W complex which carry a positive charge, the interaction of the complex with PEG and PVP will be via hydrogen bonds O···H and N···H.

Collagen is one of the most abundant proteins in the human body, and, compared to all others, it makes up 40 % of the total mass. In the skin, that percentage is much higher, almost 75 %. The three main amino acids, glycine, proline and lysine participate in its formation. Depending on the order of amino acids, there are about 28 different types of collagen. It is extremely important for the healthy appearance of the skin, because it's a support, together with elastin network, that allows the skin to return to it's original position after being deformed by movement. With age, as the amount of collagen fibres in the skin decreases, and due to the effects of UV and high-energy photons of the sun, pollution, age and so on, skin deteriorates significantly, and constant movement in the same place on the skin leads to changes called wrinkles. Until now to activate collagen and elastin in an optimal way 3HFWC-W substance was used, which acts on the biological structures that are arranged according to the same laws of symmetry (collagen, clathrin, microtubules, centrioles, flagella and processes based on Gibbs free energy), harmonises them, and brings them into a natural functional state. Due to its icosahedral structure, it has appropriate vibrational-rotational states that enable its harmonisation. Namely, 3HFWC-W stimulates the formation of linearly bound water molecules in accordance with icosahedral (Fibonacci) properties. This mechanism takes place in several steps: (i) Establishing the original state with the conformational structure of biomolecules on the water/hydrogen bond and thus achieving the optimal state; (ii) Signal transmission via non-covalent hydrogen bonds in the α-helix via peptide planes; (iii) Reaction of a liquid crystal structure in a cosmetic product applied to the skin; (iv) Creation of a water cluster with icosahedral symmetry, which together with water organised in linear chains, that creates a network of water with properties of icosahedral symmetry [2].

Previous studies have confirmed that 3HFWC-W increases the moisture content and stimulates the regeneration of biomolecules. In comparison with four commercial cosmetic products, the 3HFWC-W based creams showed better effects by 12-32 % [22]. Nanoparticles usually have different physical, catalytic or biological properties from larger materials with the same chemical composition. The key to achieving better nanoparticle performance is increasing the surface to volume ratio of the material, due to reduction to nanometre dimensions. The large and reactive interface is responsible for the catalytic, antimicrobial and many electronic properties that give nanoparticles a significant advantage over bulk materials. The most important difference between basic materials and nanoparticles is that they have a large number of atoms on a small outer surface, which leads to high surface energy and high reactivity. Ease of production and functionalisation have resulted in various applications in many fields of biomedicine, such as nanosensors, targeted drug delivery, medical imaging, but also in the cosmetics industry. The high optical absorption of AuNPs, their scattering properties and low or complete lack of toxicity have made them a promising class of ingredient in cosmetics. Previous research has shown that the main properties of AuNPs in beauty care are accelerating blood circulation, anti-inflammatory properties, antiseptic properties, increasing the firmness and elasticity of the skin, improving the metabolism, and, thus, slowing down the ageing process [54]**.** Testing of creams with the quantum substance 3HFWC-W based on the double derivative of C_{60} molecules was conducted, in order to investigate the impact of the synergistic effects of C_{60} and AuNPs. To see whether there is a synergistic effect of AuNPs and the substance 3HFWC-W, we monitored changes in the forearms of the subjects (women) in two places every seven days. Wanting to see how the creams with AuNPs (group III) and with the added 3HFWC-W (group IV) affected collagen, we observed red light, because it penetrates to the depths where collagen is formed.

A more detailed mechanism of the 3HFWC-W$^{AuNA\ PEG20}$ substance of the cream in the skin is presented in Fig. 12. The mechanism is as follows:

a) The 3HFWC-W$^{AuNA\ PEG20}$ substance penetrates through the layers of the epidermis up to the basement membrane, where, under the oscillatory processes of collagen in the basement membrane, it is activated and acts on the fibroblasts. Synthesis of new collagen and elastin through water channels takes place, then continues to pass through the epidermis to the skin`s surface, releasing water molecules from the peripheral water layers of the substance.
b) Trans Epidermal Water Loss is being implemented, which affects the length of the segments of lipid layers and regulates the amount of water leaving the epidermis.
c) Regulation of the collagen oscillatory processes occurs in the basement membrane, and, with that, the preservation of its stability is maintained.
d) In the final stage activation of the fibroblasts in the dermis from the basement membrane occurs, using water (organised in water chains), which leads to the synthesis of new collagen and elastin.

Based on the obtained scientific results the new substance 3HFWC-W with AuNPs will be prepared in a cream with the name La Danza-Hyperlight fusion Anti - Ageing essential complex. This will be followed by extensive testing to ensure maximum safety for cosmetic users.

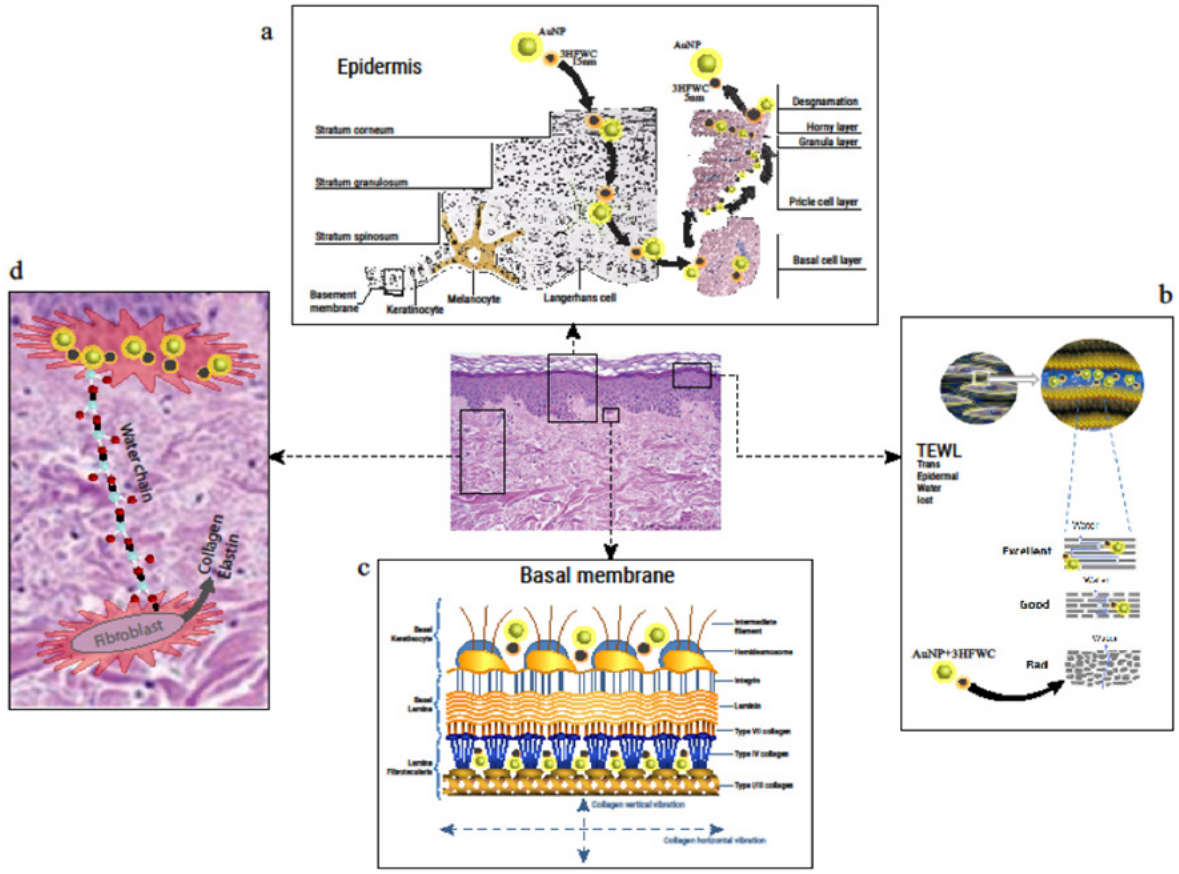

Fig. 12 Schematic representation of the effect of the 3HFWC-W$^{AuNA\ PEG20}$ substance in the epidermis a) and b) on the basement membrane c) and in the dermis, from the basal membrane to fibroblast, via water hydrogen bonds, for d) a new collagen synthesis

5. Conclusion

Within the performed research, we came to the following findings:

- With the use of Ultrasonic Spray Pyrolysis and freeze drying, AuNPs were successfully synthesised, with the selected stabilisers that prevented their agglomeration. Dry AuNPs had the final properties required for the preparation of cosmetic creams.
- The use of a PVP stabiliser in the freeze drying process allowed the formation of a very stable form of dried AuNPs, with a smaller shrinkage observed in the drying Miron glass cosmetic jar compared to the PEG stabiliser. Measurements showed that PVP helped reduce the surface charge of AuNPs in suspension, which allowed for better 3HFWC-W setting around the surface of the AuNPs.
- The results of the six weeks clinical study cream on volunteers found improvements of collagen quality in skin between 18-24 %, achieved due to the use of AuNPs (groups I, II, III) in a standard cream base, while the cream with the combination of 3HFWC-W and AuNPs gave significantly higher improvements with the value of 45.7 %.
- It was also discovered that hydration of the skin (*stratum cornum*) increased by 6.4 -9.6 % in standard creams with AuNPs, and 73.7 % in the 3HFWC-W/AuNPs cream. Similar results were measured by the epidermis-dermis function, where 24-28 % for standard creams with AuNPs was identified, and 38.4 % for the cream 3HFWC-W/AuNPs.

Acknowledgments

This research was funded by the Slovenian Research Agency, Research Core Funding No. P2-0120 and I0-0029 and the Serbian Serbian Research Agency, Research Core Funding No. III 41009 (2019).

References

[1] Krutmann, J. (2003). Hautalterung, *Der Hautarzt,* Vol. 54, No. 9, 803-803, doi: 10.1007/s00105-003-0610-6.
[2] Miljkovic, S., Jeftic, B., Stankovic, I., Stojiljkovic, I., Koruga, D. (2021). Mechanisms of skin moisturization with hyperharmonized hydroxyl modified fullerene substance, *Journal of Cosmetic Dermatology,* Vol. 20, No. 9, 3018-3025, doi: 10.1111/jocd.13965.
[3] Pulit-Prociak, J., Grabowska, A., Chwastowski, J., Majka, T.M., Banach, M. (2019). Safety of the application of nanosilver and nanogold in topical cosmetic preparations, *Colloids and Surfaces B: Biointerfaces,* Vol. 183, Article No. 110416, doi: 10.1016/j.colsurfb.2019.110416.
[4] Gupta, R., Rai, B. (2017). Effect of size and surface charge of gold nanoparticles on their skin permeability: A molecular dynamics study, *Scientific Reports*, Vol. 7, Article No. 45292, doi: 10.1038/srep45292.
[5] Manatunga, D.C., Godakanda, V.U., Herath, H.M.L.P. B, de Silva, R.M., Yeh, C.-Y., Chen, J.-Y., de Silva, A.A.A., Rajapaksha, S., Nilmini, R., de Silva, K.M.N. (2020). Nanofibrous cosmetic face mask for transdermal delivery of nano gold: Synthesis, characterization, release and zebra fish employed toxicity studies, *Royal Society Open Science,* Vol. 7, Article No. 201266, doi: 10.1098/rsos.201266.
[6] Bachelet, M. (2016). Design of pH-responsive gold nanoparticles in oncology, *Materials Science and Technology,* Vol. 32, No. 8, 794-804, doi: 10.1179/1743284715Y.0000000090.
[7] Banstola, A., Emami, F., Jeong, J.-H., Yook, S. (2018). Current applications of gold nanoparticles for medical imaging and as treatment agents for managing pancreatic cancer, *Macromolecular Research,* Vol. 26, No. 11, 955-964, doi: 10.1007/s13233-018-6139-4.
[8] Yupapin, P., Suwandee, P. (2016). Nano-particles for cosmetic use: Particle sizing, cytotoxicity test, and facial gesture monitoring model, *Journal of Cosmetology & Trichology,* Vol. 2, No. 2, Article No. 112, doi: 10.4172/2471-9323.1000112.
[9] Kaul, S., Gulati, N., Verma, D., Mukherjee, S., Nagaich, U. (2018). Role of nanotechnology in cosmeceuticals: A review of recent advances, *Journal of Pharmaceutics,* Vol. 2018, Article ID 3420204, doi: 10.1155/2018/3420204.
[10] Kim, J.-H., Hong, C.-O., Koo, Y.-C., Choi, H.-D., Lee, K.-W. (2012). Anti-glycation effect of gold nanoparticles on collagen, *Biological and Pharmaceutical Bulletin,* Vol. 35, No. 2, 260-264, doi: 10.1248/bpb.35.260.
[11] Fytianos, G., Rahdar, A., Kyzas, G.Z. (2020). Nanomaterials in cosmetics: Recent updates, *Nanomaterials,* Vol. 10, No. 5, Article No. 979, doi: 10.3390/nano10050979.
[12] Lieber, C.M., Chen, C.-C. (1994). Preparation of fullerenes and fullerene-based materials, *Solid State Physics,* Vol. 48, 109-148, doi: 10.1016/S0081-1947(08)60578-0.
[13] Matija, L., Tsenkova, R., Munćan, J., Miyazaki, M., Banba, K., Tomić, M., Jeftić, B. (2013). Fullerene based nanomaterials for biomedical applications: Engineering, functionalization and characterization, *Advanced Materials Research,* Vol. 633, 224-238, doi: 10.4028/www.scientific.net/AMR.633.224.

[14] Milani, M., Sparavigna, A. (2017). The 24-hour skin hydration and barrier function effects of a hyaluronic 1%, glycerin 5%, and Centella asiatica stem cells extract moisturizing fluid: An intra-subject, randomized, assessor-blinded study, *Clinical, Cosmetic and Investigational Dermatology,* Vol. 10, 311-315, doi: 10.2147/CCID.S144180.
[15] Marinković, K., Gomez, L.S., Rabanal, M.E., Mančić, L., Milošević, O. (2010). Aerosol route in processing of nanostructured phosphor materials, *Processing and Application of Ceramics,* Vol. 4, No. 3, 135-145, doi: 10.2298/pac1003135m.
[16] Majerič, P., Rudolf, R. (2020). Advances in ultrasonic spray pyrolysis processing of noble metal nanoparticles–Review, *Materials,* Vol. 13, No. 16, Article No. 3485, doi: 10.3390/ma13163485.
[17] Ravnik, J., Golobič, I., Sitar, A., Avanzo, M., Irman, Š., Kočevar, K., Cegnar, M., Zadravec, M., Ramšak, M., Hriberšek, M. (2018). Lyophilization model of mannitol water solution in a laboratory scale lyophilizer, *Journal of Drug Delivery Science and Technology,* Vol. 45, 28-38, doi: 10.1016/j.jddst.2018.02.015.
[18] Cui, Y., Wu, Q., He, J., Li, M., Zhang, Z., Qiu, Y. (2020). Porous nano-minerals substituted apatite/chitin/pectin nanocomposites scaffolds for bone tissue engineering, *Arabian Journal of Chemistry,* Vol. 13, No. 10, 7418-7429, doi: 10.1016/j.arabjc.2020.08.018.
[19] Chang, Y., Zheng, C., Chinnathambi, A., Alahmadi, T.A., Alharbi, S.A. (2021). Cytotoxicity, anti-acute leukemia, and antioxidant properties of gold nanoparticles green-synthesized using Cannabis sativa L leaf aqueous extract, *Arabian Journal of Chemistry,* Vol. 14, No. 4, Article No. 103060, doi: 10.1016/j.arabjc.2021.103060.
[20] Koruga, D. (2011). *Composition of matter containing harmonized hydroxyl modified fullerene substance,* Patent US 8058483 B52, from *https://patents.google.com/patent/US8058483*, accessed December 18, 2021.
[21] Koruga, D. (2019). *Compositions comprising hyper harmonized hydroxyl modified fullerene substances*, Patent App. No. PCT/EP2019/083307, Int. Pub. No.:WO 2021/110234 A1, 2021, from *https://patents.google.com/patent/WO2021110234A1/en*, accessed December 18, 2021.
[22] Matija, L., Koruga, D., Jovanović, J., Dobrosavljević, D., Ignjatović, N. (2004). In vitro and in vivo investigation of collagen – C60(OH)24 interaction, *Materials Science Forum,* Vol. 453-454, 561-566, doi: 10.4028/www.scientific.net/msf.453-454.561.
[23] Miljković, N., Godman, B., Kovačević, M., Polidori, P., Tzimis, L., Hoppe-Tichy, T., Saar, M., Antofie, I., Horvath, L., De Rijdt, T., Vida, R.G., Kkolou, E., Preece, D., Tubić, B., Peppard, J., Martinez, A., Yubero, C.G., Haddad, R., Rajinac, D., Zelić, P., Jenzer, H., Tartar, F., Gitler, G., Jeske, M., Davidescu, M., Beraud, G., Kuruc-Polje, D., Haag, K.S., Fischer, H., Sviestina, I., Ljubojević, G., Markestad, A., Vujić-Aleksić, V., Nežić, L., Crkvenčič, A., Linnolahti, J., Ašanin, B., Duborija-Kovačević, N., Bochenek, T., Huys, I., Miljković, B. (2020). Prospective risk assessment of medicine shortages in Europe and Israel: Findings and implications, *Frontiers in Pharmacology,* Vol. 11, Article No. 357, doi: 10.3389/fphar.2020.00357.
[24] Rudolf, R., Friedrich, B., Stopić, S., Anžel, I., Tomić, S., Čolić, M. (2012). Cytotoxicity of gold nanoparticles prepared by ultrasonic spray pyrolysis, *Journal of Biomaterials Applications,* Vol. 26, No. 5, 595-612, doi: 10.1177/0885328210377536 .
[25] Rudolf, R., Majerič, P., Tomić, S., Shariq, M., Ferčec, U., Budič, B., Friedrich, B. Vučević, D., Čolić, M. (2017). Morphology, aggregation properties, cytocompatibility, and anti-inflammatory potential of citrate-stabilized AuNPs prepared by modular ultrasonic spray pyrolysis, *Journal of Nanomaterials*, Vol. 2017, Article ID 9365012, doi: 10.1155/2017/9365012.
[26] Rudolf, R., Majerič, P., Štager, B. Albreht, B. (2020). *Process for the production of gold nanoparticles by modified ultrasonic spray pyrolysis:* patent application no. P-202000079. Ljubljana: Office of the Republic of Slovenia for Intellectual Property, Slovenia, Ljubljana: Urad RS za intelektualno lastnino.
[27] Shariq, M., Chattopadhyaya, S., Rudolf, R., Dixit, A.R. (2020). Characterization of AuNPs based ink for inkjet printing of low cost paper based sensors, *Materials Letters,* Vol. 264, Article ID 127332, doi: 10.1016/j.matlet.2020.127332.
[28] Shariq, M., Friedrich, B., Budic, B., Hodnik, N., Ruiz-Zepeda, F., Majerič, P., Rudolf, R. (2018). Successful synthesis of gold nanoparticles through ultrasonic spray pyrolysis from a gold(III) nitrate precursor and their interaction with a high electron beam, *ChemistryOpen,* Vol. 7, No. 7, 533-542, doi: 10.1002/open.201800101.
[29] Abdelwahed, W., Degobert, G., Stainmesse, S., Fessi, H. (2006). Freeze-drying of nanoparticles: Formulation, process and storage considerations, *Advanced Drug Delivery Reviews,* Vol. 58, No. 15, 1688-1713, doi: 10.1016/j.addr.2006.09.017.
[30] Jović, Z. (2020). *Quantum cosmetics – Revolution in skin care,* Nova Galaksija – Zepter's Nanoworld, 86-98.
[31] Koruga, Đ., Miljković, S., Ribar, S., Matija, L., Kojić, D. (2010). Water hydrogen bonds study by opto-magnetic fingerprint technique, *Acta Physica Polonica A,* Vol. 117, No. 5, 777-781, doi: 10.12693/APhysPolA.117.777.
[32] Koruga, Đ., Bandić, J., Janjić, G., Lalović, Č., Munćan, J., Dobrosavljević Vukojević, D. (2012). Epidermal layers characterisation by opto-magnetic spectroscopy based on digital image of skin, *Acta Physica Polonica A,* Vol. 121, No. 3, 606-610, doi: 10.12693/APhysPolA.121.606.
[33] Jeftic, B., Papic-Obradovic, M., Muncan, J., Matija, L., Koruga, D. (2017). Optomagnetic imaging spectroscopy application in cervical dysplasia and cancer detection: Comparation of stained and unstained papanicolaou smears, *Journal of Medical and Biological Engineering,* Vol. 37, No. 6, 936-943, doi: 10.1007/s40846-017-0255-z.
[34] Dragicevic, A., Matija, L., Krivokapic, Z., Dimitrijevic, I., Baros, M., Koruga, D. (2019). Classification of healthy and cancer states of colon epithelial tissues using opto-magnetic imaging spectroscopy, *Journal of Medical and Biological Engineering*, Vol. 39, No. 3, 367-380, doi: 10.1007/s40846-018-0414-x.
[35] Koruga, D., Tomic, A. (2009). *System and method for analysis of light-matter interaction based on spectral convolution,* Int. App. NoL. PCT/US2009/030347, Int. Pb. No.: WO 2009/089292 A1, 2009.

[36] Bandic, J., Koruga, D., Marinkovich, S., Mehendale, R. (2007). *Analytic methods of tissue evaluation,* Patent US 10,085,643 B2, 2018.
[37] Jacques, S.L. (2013). Optical properties of biological tissues: A review, *Physics in Medicine & Biology,* Vol. 58, No. 11, R37-61, doi: 10.1088/0031-9155/58/11/R37.
[38] Higuchi, T. (1988). Approach to an irregular time series on the basis of the fractal theory, *Physica D: Nonlinear Phenomena,* Vol. 31, No. 2, 277-283, doi: 10.1016/0167-2789(88)90081-4.
[39] Klonowski, W. (2002). Chaotic dynamics applied to signal complexity in phase space and in time domain, *Chaos, Solitons & Fractals,* Vol. 14, No. 9, 1379-1387, doi: 10.1016/S0960-0779(02)00056-5.
[40] Lin, P.-C, Lin, S., Wang, P.C., Sridhar, R. (2014). Techniques for physicochemical characterization of nanomaterials, *Biotechnology Advances,* Vol. 32, No. 4, 711-726, doi: 10.1016/j.biotechadv.2013.11.006.
[41] Tsantilis, S., Pratsinis, S.E. (2004). Soft- and hard-agglomerate aerosols made at high temperatures, *Langmuir,* Vol. 20, No. 14, 5933-5939, doi: 10.1021/la036389w.
[42] Yeap, S.P. (2018). Permanent agglomerates in powdered nanoparticles: Formation and future prospects, *Powder Technology,* Vol. 323, 51-59, doi: 10.1016/j.powtec.2017.09.042.
[43] Teleki, A., Wengeler, R., Wengeler, L, Nirschl, H., Pratsinis, S.E. (2008). Distinguishing between aggregates and agglomerates of flame-made TiO2 by high-pressure dispersion, *Powder Technology,* Vol. 181, No. 3, 292-300, doi: 10.1016/j.powtec.2007.05.016.
[44] Behera, M., Ram, S. (2013). Spectroscopy-based study on the interaction between gold nanoparticle and poly(vinylpyrrolidone) molecules in a non-hydrocolloid, *International Nano Letters,* Vol. 3, Article No. 17, doi: 10.1186/2228-5326-3-17.
[45] Seoudi, R. Fouda, A.A., Elmenshawy, D.A. (2010). Synthesis, characterization and vibrational spectroscopic studies of different particle size of gold nanoparticle capped with polyvinylpyrrolidone, *Physica B: Condensed Matter*, Vol. 405, No. 3, 906-911, doi: 10.1016/j.physb.2009.10.012.
[46] Tiyyagura, H.R., Majerič, P., Bračič, M., Anžel, I., Rudolf, R. (2021). Gold inks for inkjet printing on photo paper: Complementary characterisation, *Nanomaterials,* Vol. 11, No. 3, Article No. 599, doi: 10.3390/nano11030599.
[47] Majerič, P. (2016). *Synthesis of gold nanoparticles with a modified ultrasonic spray pyrolysis,* Doctoral dissertation, University of Maribor, Faculty of Mechanical Engineering.
[48] Sumi, N., Chitra, K.C. (2019). Impact of fullerene C_{60} on behavioral and hematological changes in the freshwater fish, Anabas testudineus (Bloch, 1792), *Applied Nanoscience,* Vol. 9, No. 8, 2147-2167, doi: 10.1007/s13204-019-01041-1.
[49] Wang, X., Tang, F., Qi, X., Lin, Z., Battocchi, D., Chen, X. (2019). Enhanced protective coatings based on nanoparticle fullerene C_{60} for oil & gas pipeline corrosion mitigation, *Nanomaterials,* Vol. 9, No. 10, Article No. 1476, doi: 10.3390/nano9101476.
[50] Holec, D., Löfler, L., Zickler, G.A., Vollath, D., Fischer, F.D. (2021). Surface stress of gold nanoparticles revisited, *International Journal of Solids and Structures,* Vol. 224, Article No. 111044, doi: 10.1016/j.ijsolstr.2021.111044.
[51] Rudolf, R., Majerič, P., Golub, D., Tiyyagura, H.R. (2020). Testing of novel nano gold ink for inkjet printing, *Advances in Production Engineering & Management,* Vol. 15, No. 3, 358-368, doi: 10.14743/apem2020.3.371.
[52] Gawade, R.P., Chinke, S.L., Alegaonkar, P.S. (2020). Chapter 17 - Polymers in cosmetics, *Polymer Science and Innovative Applications,* Elsevier, Amsterdam, Netherlands, 545-565, doi: 10.1016/B978-0-12-816808-0.00017-2.
[53] Al-Johani, H., Abou-Hamad, E., Jedidi, A., Widdifield, C.M., Viger-Gravel, J., Sangaru, S.S., Gajan, D., Anjum, D.H., Ould-Chikh, S., Hedhili, M.N., Gurinov, A., Kelly, M.J., El Eter, M., Cavallo, L., Emsley, L., Basset, J.-M. (2017). The structure and binding mode of citrate in the stabilization of gold nanoparticles, *Nature Chemistry,* Vol. 9, 890-895, doi: 10.1038/nchem.2752.
[54] Prajapati, P. (2011). Overview on applications of nanoparticles in cosmetics, *Asian Journal of Pharmaceutical and Clinical Research,* Vol. 1, Article No. 40.

Appendix A

List of abbreviations

AuNC PEG10	AuNPs prepared by USP, with a chloride precursor with a concentration 0.5 g/L Au and collected in a suspension of D.I. water with 10 g/L PEG
AuNA PEG20	AuNPs prepared by USP, with an acetate precursor with a concetration 0.5 g/L Au and collected in a suspension of D.I. water with 20 g/L PEG
AuNC PVP5	AuNPs prepared by USP, with a chloride precursor with a concentration 0.5 g/L Au and collected in a suspension of D.I. water with 5 g/L PVP
AuNPs	Gold nanoparticles
D.I. water	Deionised water
DLS	Dynamic Light Scattering
EDS	Energy-Dispersive X-ray Spectroscopy
HFD	Higuchi Fractal Dimension

HDF	Human dermal fibroblasts
ICP-MS	Inductively Coupled Plasma-Mass Spectrometry
LED	Light-Emitting Diode
NHS	Nano-harmonised substance
OMIS	Opto-Magnetic Imaging Spectroscopy
PEG	Polyethylene glycol
PVP	Polyvinylpyrrolidone
RI	Refractive Index
SEM	Scanning Electron Microscopy
TEM	Transmission Electron Microscopy
USP	Ultrasonic Spray Pyrolysis
wB	Blue channel of white LED light
wG	Green channel of white LED light
WLD	wavelength difference
wR	Red channel of white LED light
w(G-B)	Green minus Blue channel of white LED light (diffuse)
w(R-B)	Red minus Blue channel of white LED light (diffuse)
w(R-G)	Red minus Green channel of white LED light (diffuse)
3HFWC-W	Hyper Harmonised Hydroxyl Modified Fullerene